Available online at www.sciencedirect.com
ScienceDirect
Cement and Concrete Research 37 (2007) 528–536
Cement and Concrete Research

Effects of setting regulators on the efficiency of an inorganic acid based alkali-free accelerator reacting with a Portland cement

C. Maltese *, C. Pistolesi, A. Bravo, F. Cella, T. Cerulli, D. Salvioni

Mapei S.p.A. — Via Cafiero, 22-20158 Milan, Italy

Received 6 July 2005; accepted 11 January 2007

Abstract

Today, in the field of underground constructions, alkali-free accelerators are commonly employed, during tunnel excavation, to allow flash concrete setting. In this way, the cementitious sprayed material can firmly bond to the tunnel walls, controlling the convergence (the tendency of the section to squeeze). Their efficiency may be related to many parameters like: cement type, setting regulator, concrete composition, working temperature. Nevertheless, the influence of such factors on the accelerator performance has not been clarified yet. The accelerator efficacy is evaluated by real spraying test in job site or, when only laboratory equipment are available, by measuring the final setting times of cement systems admixed with the accelerator. Several alkali-free flash setting admixtures are available on the market. They can be divided into two main categories both containing aluminium sulphate complexes stabilized either by inorganic acids or by organic acids. In this paper, the influence of different setting regulators on the performances of an inorganic acid based alkali-free accelerator was analysed. Portland cement samples were obtained by mixing clinker with gypsum, α-hemihydrate, β-hemihydrate or anhydrite. The setting regulator instantaneous dissolution rates were evaluated through conductivity measurements. The setting time of cement pastes with and without the accelerator was measured. It was found that the shorter the final setting time (therefore the more efficient is the accelerator) the lower the setting regulator instantaneous dissolution rate. In order to understand this phenomenon, a comparison was performed between accelerated cement paste samples containing the setting regulator with the highest (β-hemihydrate) and the lowest instantaneous dissolution rate (anhydrite). The analytical work included morphological (Environmental Scanning Electron Microscopy–Field Emission Gun — ESEM–FEG), crystal–chemical (X-Ray Powder Diffraction — XRD), physical–chemical (hydration temperature profile) and chemical (Induced Coupled Plasma–Atomic Emission Spectroscopy — ICP/AES) evaluations. The results revealed significant morphological differences among the investigated samples.

Keywords: Acceleration; Ettringite; Alkali-free accelerator

1. Introduction

Alkali-free accelerators are relatively new liquid concrete admixtures used in the area of underground constructions [1–5]. In the European market they are replacing the classical alkali-rich accelerators, like sodium aluminate or sodium silicate water based solutions, being safer chemicals. Furthermore, the concrete sprayed with these new alkali-free accelerators can reach higher long term compressive strengths [6]. The accelerating admixtures cause a fast concrete setting allowing projecting the cementitious material onto the rock wall. The concrete lining acts as a consolidating shield useful to control the tunnel convergences [7].

Several alkali-free accelerators are available on the market. They can be divided in two main categories both containing aluminium sulphate complexes, which are stabilized either by

Table 1
Cement paste compositions (expressed as % by mass)

Sample	R_{gyp}	AC_{gyp}	R_{alfa}	AC_{alfa}	R_{beta}	AC_{beta}	R_{anhd}	AC_{anhd}
Clinker	95	95	95	95	95	95	95	95
Gypsum	5	5	/	/	/	/	/	/
α-Hemihydrate	/	/	4.2	4.2	/	/	/	/
β-Hemihydrate	/	/	/	/	4.2	4.2	/	/
Anhydrite	/	/	/	/	/	/	3.95	3.95
Alkali-free accelerator	/	5	/	5	/	5	/	5
Water	45	45	45	45	45	45	45	45

* Corresponding author.
E-mail address: Building.lab@mapei.it (C. Maltese).

0008-8846/$ - see front matter © 2007 Published by Elsevier Ltd.
doi:10.1016/j.cemconres.2007.01.002

Table 2
Clinker chemical composition (expressed as % by mass)

SiO_2	Al_2O_3	Fe_2O_3	CaO	MgO
22.09+/−0.25	3.2+/−0.25	4.88+/−0.15	65.19+/−0.37	1.97+/−0.15

inorganic [8] or organic acids [9]. The capability of concrete to stick on the rock wall is related to the efficacy of the reaction between accelerator and hydrating cement. The accelerator performance can be evaluated by measuring the final setting time of accelerated mortar samples [10,11]. Several parameters could affect this reaction such as: accelerator type and its solid content [12], type and chemical composition of cement [13], setting regulator, environmental conditions, concrete temperature. Only few studies were carried out to evaluate the influence of these parameters on the accelerator reactivity. In this paper, the effects of different setting regulators on the reaction between an inorganic acid based alkali-free accelerator and a hydrating Portland cement were studied. Several cement samples were prepared by mixing clinker with some calcium sulphate phases characterised by different instantaneous dissolution rates (all expressed as grams of Ca ions in 1 l of water suspension per minute): gypsum (48 g/l min), α-hemihydrate (60 g/l min), β-hemihydrate (92 g/l min) and anhydrite (7 g/l min). These values were detected by conductivity measurements and chemical analyses of water suspensions of calcium sulphates phases [14]. Only few papers were published on the dissolution rate of calcium sulphates [15–18]. They depend strictly on several parameters like: experimental conditions (calcium sulphate concentration, mixing rate, temperature); calcium sulphate type (particle size); analytical method (conductivity; calcium selective electrode). Nevertheless, the dissolution rate order is generally accepted and the trend obtained in this paper is in agreement with the literature.

Setting times of samples composed of the above mentioned cements, water and the alkali-free accelerator were determined. The hydration of the samples with the largest differences in terms of final setting time (containing respectively β-hemihydrate and anhydrite), were followed by thermo-chemical hydration profile, ESEM–FEG (Environmental Scanning Electron Microscopy–Field Emission Gun), XRD (X-Ray Powder Diffraction) and ICP–AES (Induced Coupled Plasma–Atomic Emission Spectroscopy).

2. Experimental

Cement pastes (Table 1) were prepared according to the following procedure:

1) the quantities of clinker (from Cementi Rossi, Piacenza, Italy — Tables 2 and 3) and calcium sulphate (gypsum — from Lages, Italy, μ: 19 μm; or α-hemihydrate — from BPB, Germany, μ: 20 μm; or β-hemihydrate — from Lages, Italy, μ: 11 μm; or anhydrite — from Yesos Ibericos, Spain, μ: 8 μm; where μ is the weighted mean particle diameter) mentioned in Table 1 were homogenized in a 200 ml plastic container;
2) water (Water/Clinker=0.47) was added and stirred by a spatula for 15 s in order to obtain a homogenous slurry;
3) the mixing procedure was stopped for 1 min;
4) the inorganic acid based alkali-free accelerator (trade name Mapequick AF 1000, produced by Mapei SPA — Al_2O_3= 12% and SO_3=16%) was added and mixed for 10 s.

The resulting samples were cured at 20 °C and 95% R.H.

2.1. Instantaneous dissolution rate

The following experimental procedure was followed to calculate the instantaneous dissolution rates:

1) 0.058 mol of gypsum or α-hemihydrate or β-hemihydrate or anhydrite were added in a 350 ml plastic vessel containing 200 g of water and mixed with a magnetic stirrer (Heidolph model MR 3002) at 600 rpm;
2) conductivity of the suspensions was followed and recorded by a conductivity meter LF 538 WTO for 30 min;
3) other mixtures containing gypsum and anhydrite were prepared and after 10, 20 and 30 min, they were filtered by a filter type Schleicher and Schuell (model 597); on the resulting solution, the calcium ions concentration was measured by ICP spectroscopy (Induced Coupled Plasma Varian model Liberty 220 — each result was an average of three measurements).

2.2. Mechanical tests

The accelerator performance was evaluated by measuring initial and final setting time of the samples indicated in Table 1 (ENV 196/3 — each result is an average of three measurements).

2.3. Physical–chemical analyses

The following analyses were performed on samples R_{beta}, AC_{beta}, R_{anhd} and AC_{anhd}.

The hydration temperature profile was measured keeping the cement paste sample (0.5 kg) in a thermostatic bath (20 °C) and measuring the temperature during the first 24 h of hydration with a digital thermometer type Testo mod. 781.

The samples for ICP/AES and XRD investigations were prepared according to the following procedure:

1) At the end of the curing time (5 min, 30 min, 3 h and 20 h for ICP/AES; 30 min, 8 h and 24 h for XRD), 50 g of the cement paste was milled (Fritsch model Pulverisette 2) for 5 min;
2) The resulting powder was rapidly sieved (size: 75 μm).

Soluble ions (Al^{3+} and SO_4^{2-}) concentration was measured by ICP spectroscopy (Varian model Liberty 220) on a solution obtained by mixing for 15 min and filtering 25 g of the fine

Table 3
Phase composition according to Bogue's calculation (expressed as % by mass)

C_3S	C_2S	C_3A	C_4AF
69.0	11.4	0.2	14.9

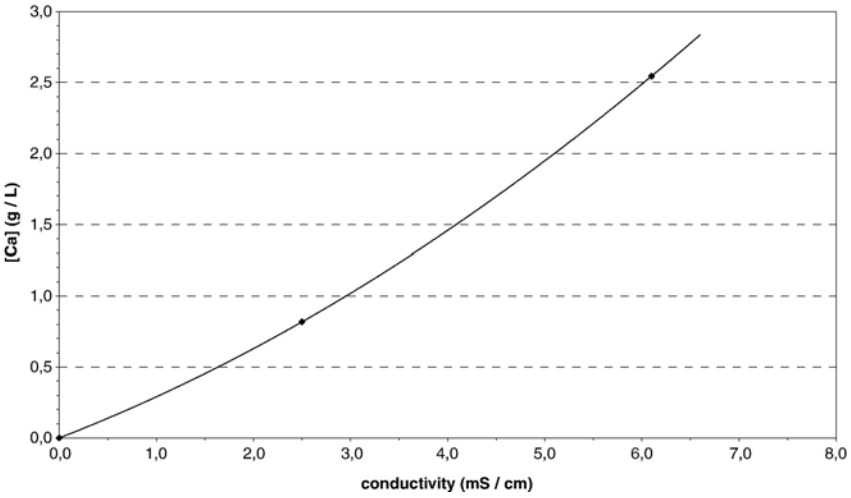

Fig. 1. Relationship concentration/conductivity.

powder in 62.5 g of water (each result is expressed as % by cement mass and is an average of three measurements).

In order to avoid the carbonation effect on young cement pastes, XRD analyses (Philips PW 1830 diffractometer with Cu (Kα) radiation) were collected on the fine powder in the range between 5° and 40° 2θ in a short time (11 min).

All these physical–chemical analyses were performed without any previous treatment to quench hydration reaction, as it has not been clarified yet if and how the use of organic solvents could modify the crystalline structure of the involved system. Therefore the sample preparation, which takes about 10 min, could have affected the results in particular during the initial hydration times (5 min and 30 min). Nevertheless, the conclusions of this paper arise from a comparison of samples subjected to identical experimental conditions and the effects of pre-treatment could be considered negligible.

2.4. Morphological analyses

An Environmental Scanning Electron Microscope (Philips mod. XL30 ESEM–FEG) was used to analyse the morphology of hydrating cement pastes. The special instrumental configuration of the ESEM–FEG allowed to work in low vacuum setting (6 Torr), with a 10 kV voltage, at a temperature of 5 °C. Therefore, the sample could be analysed in the presence of significant amounts of residual water. The study was performed till 24 h of curing.

3. Results

3.1. Instantaneous dissolution rate

For the water mixtures containing gypsum and anhydrite, it was possible to draw a curve between calcium ions concentration and conductivity (for example Fig. 1) which was used to calculate the following equation:

$$[C] = 0.0250[\mathrm{cd}]^2 + 0.265[\mathrm{cd}] \quad (\text{correlation coefficient}: \ 0.95)$$

Where

[C] calcium ions concentration (g/l);
[cd] conductivity (mS/mm).

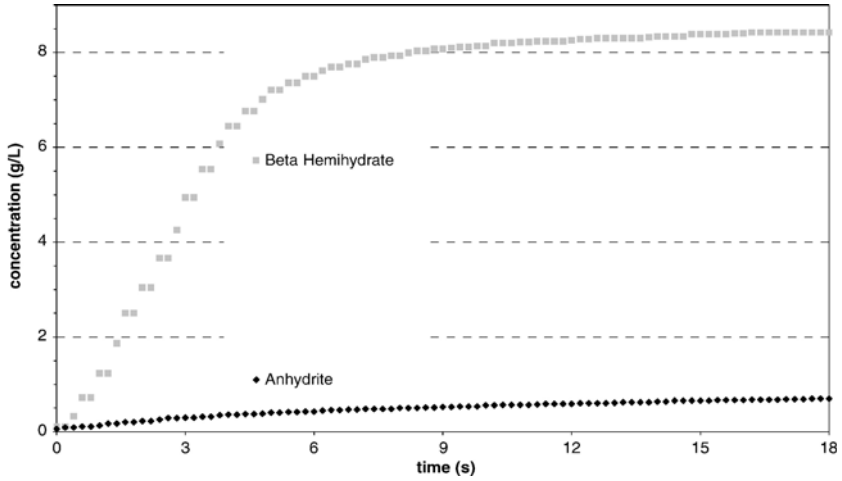

Fig. 2. Calcium ion concentration/time diagram.

Table 4
Instantaneous dissolution rate (standard deviation is indicated between brackets)

Setting regulator	Dissolution rate (as Ca ions g/l min)
Gypsum	48 (+/−5)
α-Hemihydrate	60 (+/−6)
β-Hemihydrate	92 (+/−9)
Anhydrite	7 (+/−1)

Such an equation was employed to transform the conductivity/time diagrams in concentration/time (Fig. 2). The instantaneous dissolution rates were calculated measuring the initial slope of the resulting curves (Table 4).

3.2. Mechanical tests

The results summarized in Table 5 point out that the setting regulator does not affect the final setting time of ordinary cement pastes (R_{beta}, R_{alfa}, R_{gyp}, R_{anhd}). The accelerator addition causes a significant setting time reduction (R_{alfa}, R_{gyp}, R_{anhd} compared to AC_{alfa}, AC_{gyp}, AC_{anhd} — Table 6) with the exception of the sample containing β-hemihydrate (AC_{beta}), which shows a retardation of the final setting time in comparison with its reference (R_{beta}). The data underline that the lower the setting regulator dissolution rate, the shorter the final setting time.

3.3. Physical–chemical analyses

The hydration temperature profile is related to the rate of heat release [19]. The exothermic peak observed during the first hour of curing (Fig. 3 — standard deviation: +/−0.5 °C) is due to an early cement hydration and hydrated sulphoaluminates formation. On the contrary, the second peak (between 2 and 20 h) is associated to C_3S hydration, which produces C–S–H and portlandite. Commonly, during this stage, also known as acceleratory period, the final setting time of ordinary cementitious systems occurs. Fig. 3 shows an increase of the first peak height on the cement pastes admixed with the alkali-free accelerator (AC_{beta} and AC_{anhd} in comparison with R_{beta} and R_{anhd}) due to aluminium sulphate, contained in the alkali-free accelerator, which supplies a considerable amount of aluminium and sulphate ions to the cementitious pore solution, thus favouring a massive sulphoaluminates formation. Such a peak intensity increase, due to the use of alkali-free accelerators, was already observed [20]. AC_{beta} and AC_{anhd} have similar behaviours. The samples admixed with the flash setting admixture are characterised by a retarded acceleratory period. The effect is more pronounced for AC_{beta}, thus confirming its retarded final setting with respect to its reference (R_{beta}).

ICP/AES analyses do not reveal aluminium ions in the samples. Likely, they are immediately and totally consumed to give insoluble hydrated sulphoaluminates.

During the first hydration instants, a rapid decrease of soluble sulphates is visible in the sample containing β-hemihydrate (R_{beta} — Fig. 4). Such a behaviour is not evident in R_{anhd}. The effect could be due to a faster dissolution rate of β-hemihydrate, that produces initially a larger amount of calcium and sulphate ions, which rapidly re-hydrate to gypsum or, reacting with aluminates (present in ordinary Portland cement as C_3A or C_4AF), forming a protective layer of ettringite [21]. In these conditions, a massive formation of nucleation germs could occur. In the case of anhydrite, this dissolution process is much slower and, therefore, a slower sulphate consumption can be observed and a lower amount of nucleation germs could be originated.

Table 5
Setting time of cement pastes without the accelerator (standard deviation is indicated between brackets)

Sample	Initial / final setting time
R_{beta}	3 h 30 min / 5 h 30 min (+/−30 min)
R_{alfa}	3 h / 5 h (+/−30 min)
R_{gyp}	3 h / 5 h 30 min (+/−30 min)
R_{anhd}	3 h 30 min / 5 h 30 min (+/−30 min)

For both samples, the sulphate reduction slows down during the dormant period (from 30 min till 3 h of hydration). The coating layer of hydrated calcium sulphoaluminates could hinder further reaction between cement phases and sulphate ions.

Sample AC_{anhd} shows a faster soluble sulphate reduction compared to AC_{beta} (Fig. 5).

The XRD patterns (Figs. 6–11) show signals of crystalline ettringite in all the samples. The flash setting accelerator causes a peak height increase of ettringite (Figs. 6 and 9), as already reported in literature [20,22–24]. As time proceeds, an increase of ettringite peak intensity is visible (Figs. 6–8). The increase of ettringite peaks height as time proceeds seems less pronounced for AC_{beta} (Figs. 6–8 compared to Figs. 9–11). The accelerator slows down cement hydration. In fact, signals of portlandite are not present also after 8 h of hydration (Figs. 7 and 10). This effect could arise from the reaction between accelerator and hydrating cement giving origin to an ettringite layer on cement particles which cannot be hydrated properly.

3.4. Morphological analyses

The ESEM micrographs of the reference pastes R_{beta} and R_{anhd} show significant differences: the morphology of the sample containing β-hemihydrate is characterised by small and rounded masses (Fig. 12) whereas well shaped prismatic needles appears on the microstructure of R_{anhd} (Fig. 13). These observations support the hypothesis that a fast nucleation rate occurs in R_{beta} (for the higher instantaneous dissolution rate of β-hemihydrate) and a larger amount of gel like material could be formed. On the contrary, in R_{anhd}, for the lower instantaneous dissolution rate of anhydrite, well shaped and large hydrated

Table 6
Setting time of cement pastes containing the accelerator (standard deviation is indicated between brackets)

Sample	Initial / final setting time
AC_{beta}	2 h 30 min / 8 h 30 min (+/−30 min)
AC_{alfa}	1 min 38 s / 6 min 30 s (+/−30 s)
AC_{gyp}	1 min 6 s / 3 min 5 s (+/−20 s)
AC_{anhd}	40 s / 1 min 18 s (+/−10 s)

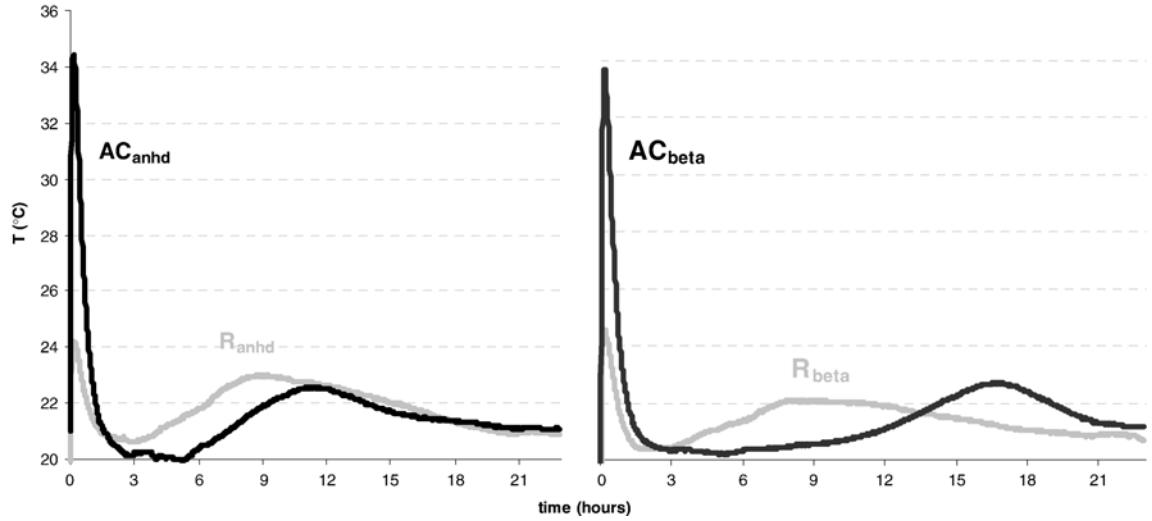

Fig. 3. Hydration temperature profiles.

calcium sulphoaluminates could be originated. As time proceeds, the morphology of the samples becomes more similar.

In Fig. 14 (ESEM micrograph of AC_{beta} after the first minute of hydration) thin large plates (likely gypsum) and smaller globular masses are present everywhere. On the contrary, at the same hydration time, the morphology of AC_{anhd} is deeply different: small rods of AFt phase are visible (Fig. 15). These differences support the presence of many nucleation germs in AC_{beta}, which promote the precipitation of gypsum and small globular masses of hydrated calcium sulphoaluminate. Whereas few nucleation germs in AC_{anhd} could favour the formation of well shaped crystals of AFt phase.

After about 3 h, in Fig. 16 (AC_{beta}) very short prismatic needles of likely ettringite are evident. At the same hydration time, the cement paste samples containing anhydrite (AC_{anhd}) show a significant growth of ettringite needles (Fig. 17).

As time proceeds (5 h and 30 min), a growth of the short prismatic rods and the formation of a gel like material is visible on AC_{beta} (Fig. 18). At the same time, AC_{anhd} does not show significant morphological variations (Fig. 19).

Only after 24 h, well formed prismatic crystals of AFt phase appear on AC_{beta} (Fig. 20).

4. Discussion

The action mechanism of alkali-free accelerators was already studied [4,6,20,22–24] and the results of this paper are in general agreement with the literature. Accelerator reacts with hydrating cement promoting a fast formation of hydrated sulphoaluminates (particularly AFt phases) thus determining a rapid viscosity increase of cement pastes which results in a shorter setting. The accelerating performances can be evaluated by determining the final setting time of cement pastes admixed with the alkali-free accelerator [6]: the shorter the final setting time, the more efficient the accelerator.

Setting of hydrating cement is influenced by the setting regulator [25] which is an anhydrous or hydrated calcium sulphate in different crystallographic forms [26]. During the first hydration stage, calcium and sulphate ions, supplied by the setting regulator, react with aluminium (normally present in cement phases like C_3A and C_4AF) and water to give an amorphous layer of aluminates with AFt phase at the edge [27], which slows down further hydration (dormant period). The morphology of such AFt phase depends on the setting regulator [27]. The accelerator is commonly added during the dormant

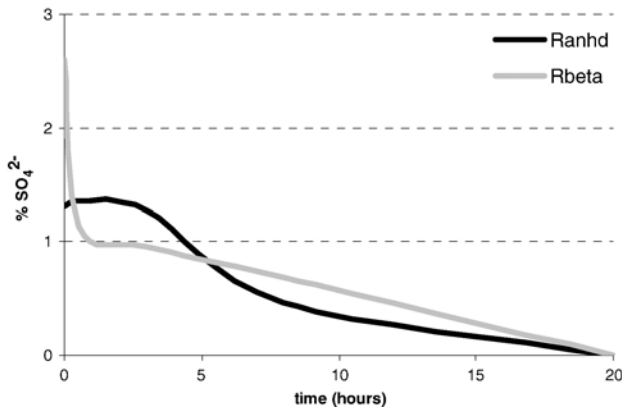

Fig. 4. Sulphate ions concentration in R_{anhd} and R_{beta}.

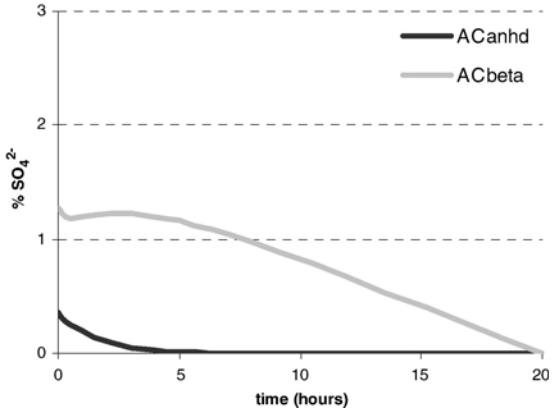

Fig. 5. Sulphate ions concentration in AC_{anhd} and AC_{beta}.

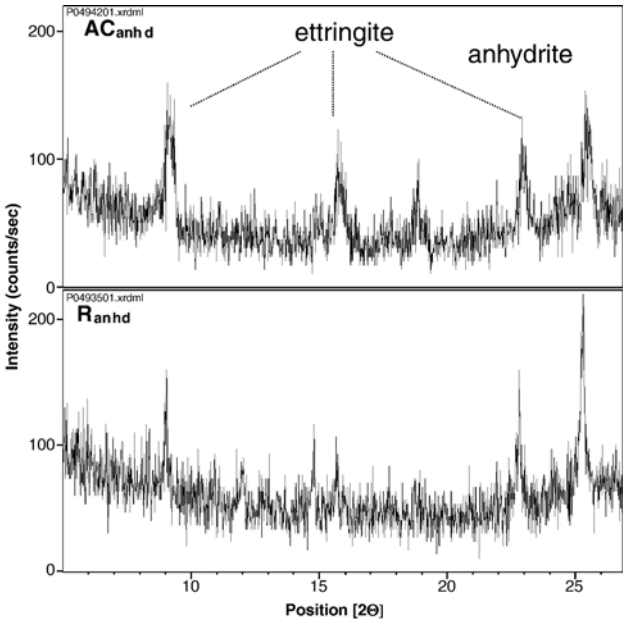

Fig. 6. XRD after 30 min of AC_{anhd} and R_{anhd}: the intensity of ettringite peaks at 9°, 15.7° and 22.9° 2θ is higher in AC_{anhd}.

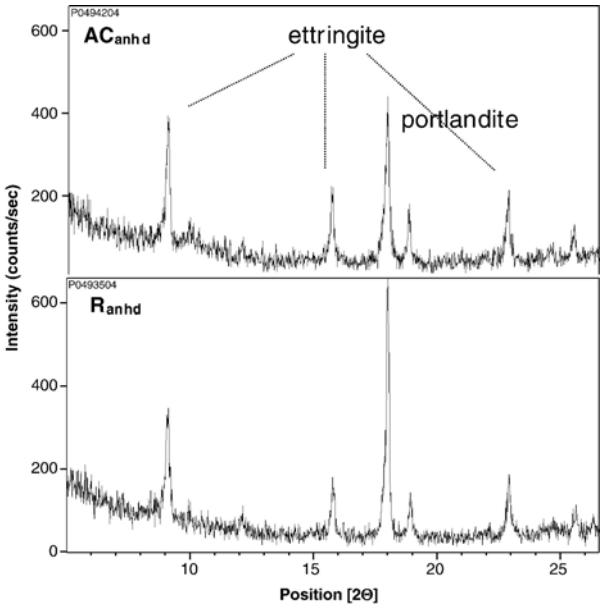

Fig. 8. XRD after 24 h of AC_{anhd} and R_{anhd}.

period, when the amorphous layer and AFt phase is already formed. The results in Tables 4 and 6 show that for cement paste samples admixed with the accelerator, the lower the setting regulator instantaneous dissolution rate (anhydrite < gypsum < α-hemihydrate < β-hemihydrate), the shorter the final setting time and, therefore, the more efficient is the accelerator. In order to explain such phenomenon, the different initial morphology between the samples containing the setting regulator with the highest dissolution rate (β-hemihydrate – R_{beta} – ESEM micrograph in Fig. 12) and the sample containing the setting regulator with the lowest dissolution rate (anhydrite – R_{anhd} – ESEM micrograph in Fig. 13) should be considered. In fact, the microstructure of R_{beta} is characterised by rounded and small masses of likely AFt phase or gypsum (due to a fast re-hydration of β-hemihydrate) which are quite different respect to the long and prismatic needles visible in R_{anhd}. These differences were already noted by Scrivener [27] studying the hydration of C_3A with gypsum and hemihydrate. When the accelerator is added, these differences could affect the kinetics of hydrated sulphoaluminate formation. In fact, the microstructures of AC_{beta}

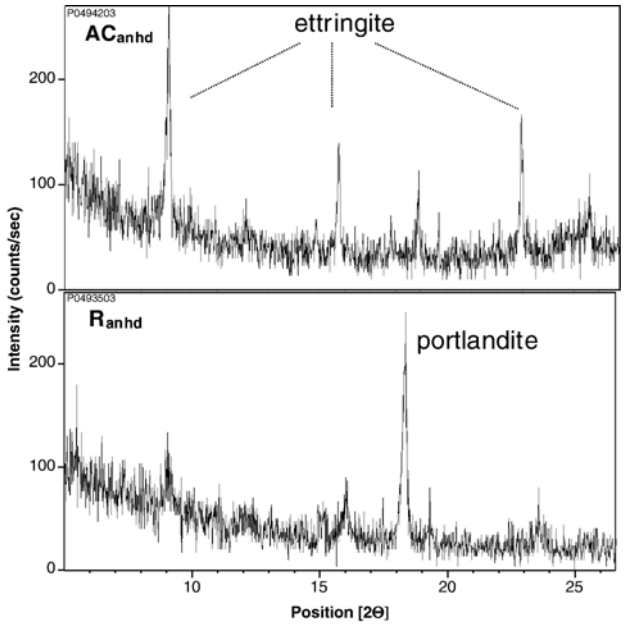

Fig. 7. XRD after 8 h of AC_{anhd} and R_{anhd}: the intensity of ettringite peaks at 9°, 15.7° and 22.9° 2θ is higher in AC_{anhd}.

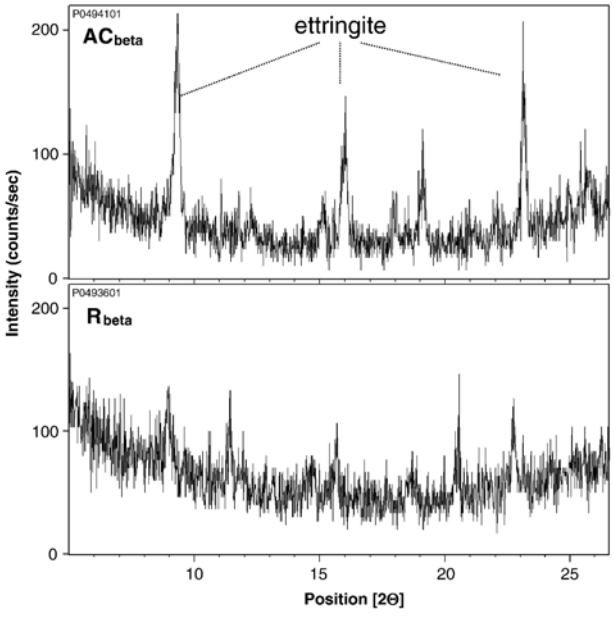

Fig. 9. XRD after 30 min of AC_{beta} and R_{beta}: the intensity of ettringite peaks at 9°, 15.7° and 22.9° 2θ is higher in AC_{beta}.

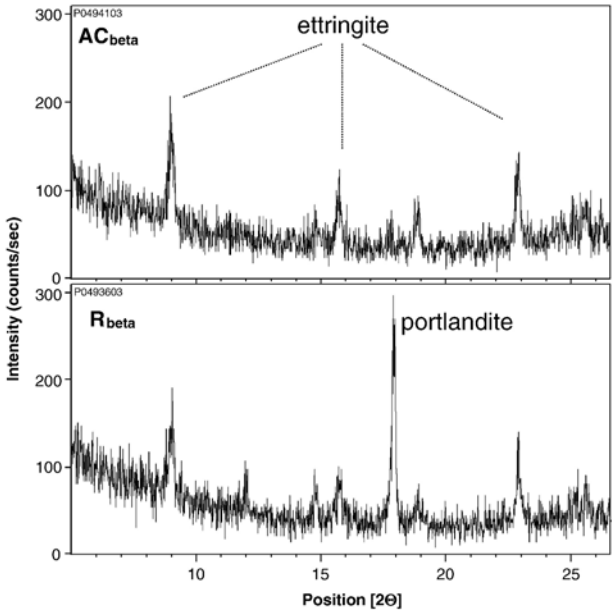

Fig. 10. XRD after 8 h of AC_{beta} and R_{beta}: the intensity of ettringite peaks at 9°, 15.7° and 22.9° 2θ is higher in AC_{beta}.

(Fig. 14) and AC_{anhd} (Fig. 15) during the first instants of cement hydration are deeply different: AC_{beta} shows large plates of possible gypsum (due to re-hydration of β-hemihydrate) and a gel like material (which could be mainly composed of hydrated calcium sulphoaluminates) whereas the micrograph of AC_{anhd} shows a compact microstructure of short prismatic needles of AFt phase. Considering that the amount of initially formed hydrated sulphoaluminates in AC_{beta} and AC_{anhd} (hydration temperature profile in Fig. 3) is similar, only the different initial microstructure of AC_{beta} and AC_{anhd} could explain their setting

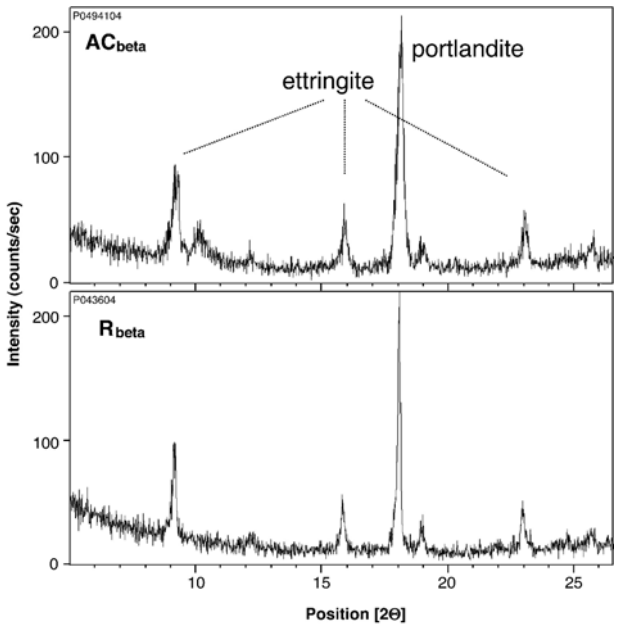

Fig. 11. XRD after 24 h of AC_{beta} and R_{beta}.

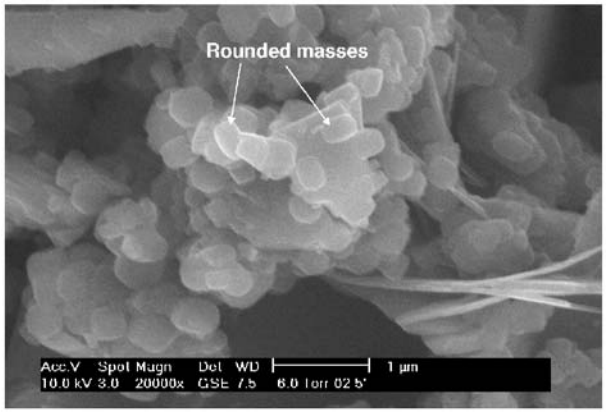

Fig. 12. ESEM micrograph of R_{beta} after 5 min of hydration (unit length 1 μm).

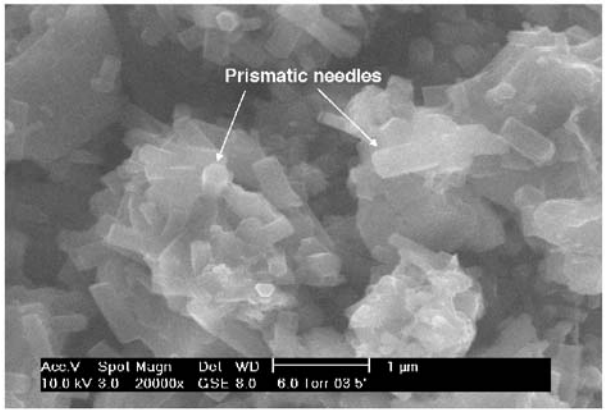

Fig. 13. ESEM micrograph of R_{anhd} after 5 min of hydration (unit length 1 μm).

behaviour. Probably, the sample containing anhydrite is characterised by a lower nucleation rate. Therefore few nucleation germs are formed, which promote a proper growth of well shaped and large ettringite crystals thus favouring a fast setting. On the contrary, the sample containing β-hemihydrate is characterised by a faster nucleation rate. Therefore many nucleation

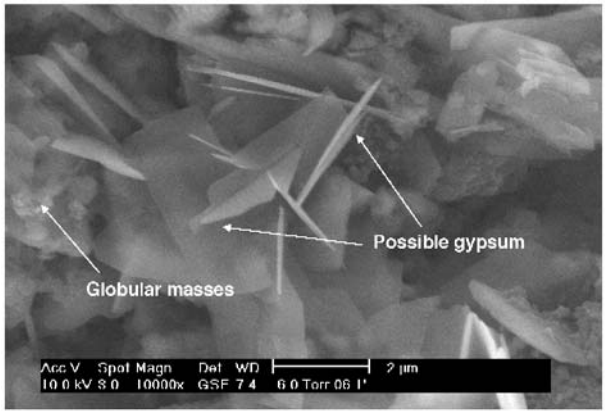

Fig. 14. ESEM micrograph of AC_{beta} after 1 min of hydration (unit length 2 μm).

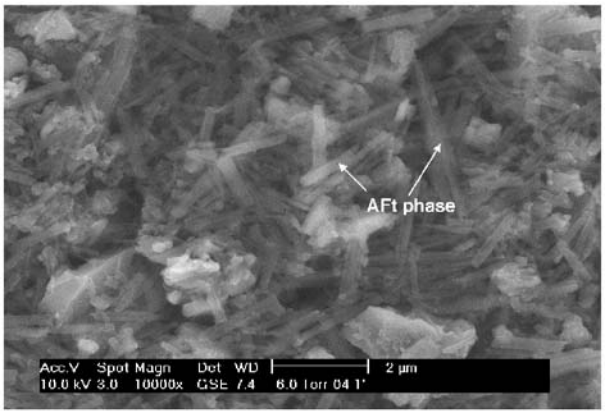

Fig. 15. ESEM micrograph of AC_{anhd} after 1 min of hydration (unit length 2 µm).

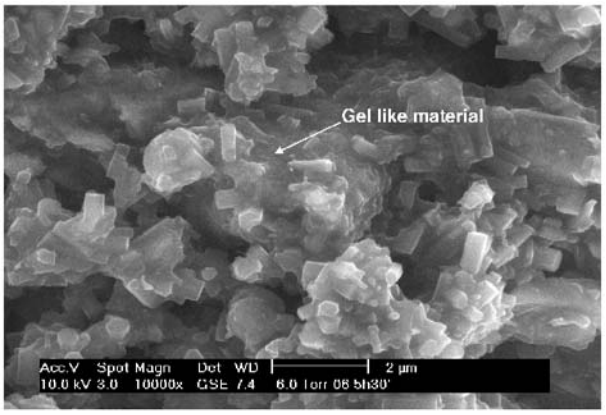

Fig. 18. ESEM micrograph of AC_{beta} 5 h and a half of hydration (unit length 2 µm).

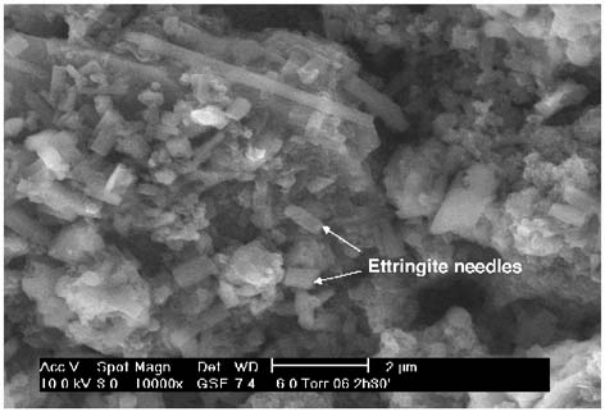

Fig. 16. ESEM micrograph of AC_{beta} after about 3 h of hydration (unit length 2 µm).

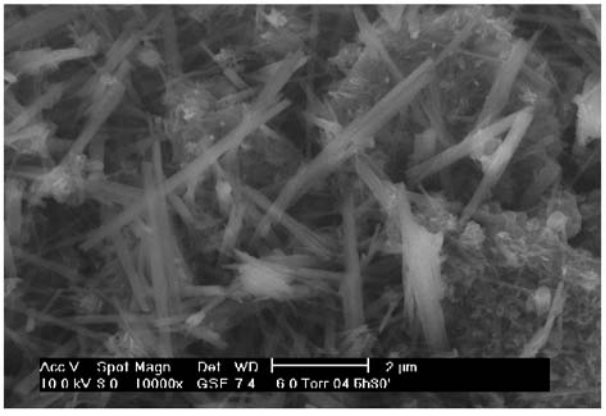

Fig. 19. ESEM micrograph of AC_{anhd} after 5 h and a half of hydration (unit length 2 µm).

germs are originated promoting a disordered and fast precipitation of gypsum or hydrated calcium sulphoaluminates in a gel like form whose consistency is too soft to allow an accelerated setting. This layer of microcrystalline or amorphous AFt phase could be a barrier for a correct C_3S hydration thus retarding a normal hydration of the cement system (the final setting time of AC_{beta} is longer than R_{beta}). Also the growth of larger ettringite crystals is much slower compared to AC_{anhd}. In fact, the XRD peak intensity of ettringite signal after 8 h is lower for AC_{beta} than AC_{anhd} (Fig. 10 compared to Fig. 7) and well shaped crystals of ettringite are only visible after 24 h of hydration (Fig. 20).

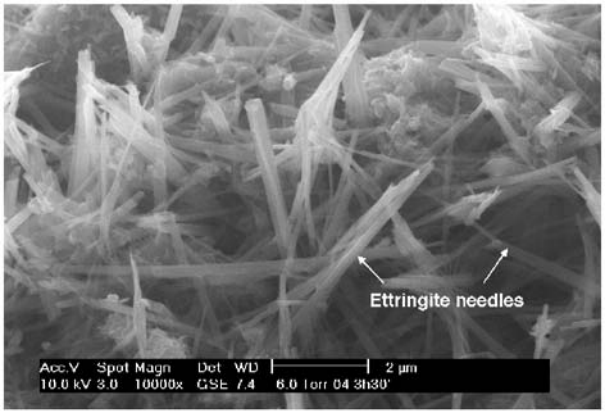

Fig. 17. ESEM micrograph of AC_{anhd} after about 3 h of hydration (unit length 2 µm).

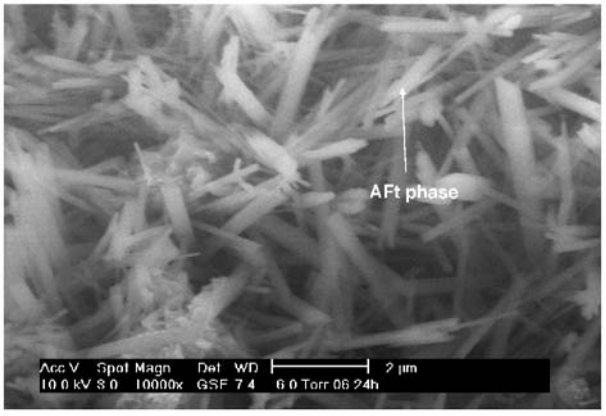

Fig. 20. ESEM micrograph of AC_{beta} 24 h of hydration (unit length 2 µm).

5. Conclusion

This study points out that the solubility rate of the setting regulators influences the reaction of an inorganic acid based alkali-free accelerator and a hydrating Portland cement. In particular, it was found that the lower the instantaneous solubility rate of the setting regulator the more efficient the accelerator. The reason for this behaviour could be connected with the different morphology of ettringite formed during the first minutes of the reaction between the hydrating cement and the alkali-free accelerator. This investigation was limited on a cement with low C_3A and one accelerator in one dosage. Furthermore the effects of α-hemihydrate were not studied in detail. Some changes in the final results could also be expected if the accelerator is added at different times after water addition. Therefore further data are necessary in order to generalize these conclusions.

Acknowledgements

We are grateful for the precious cooperation of Mr. Gurzì Pasquale of MAPEI SPA.

References

[1] R. Myrdal, Modern chemical admixtures for shotcrete, in: N. Barton, et al. (Eds.), Proc. of 3rd Symposium on Sprayed Concrete, Gol, Norway, 1999, pp. 375–382, available from www.betong.net.
[2] B. Leikauf, M. Oppliger, Alkali-free accelerators for sprayed concrete, Chimia 52 (1998) 222–224 (available from www.chimia.ch).
[3] E. Dal Negro, C. Maltese, C. Pistolesi, Use of advanced alkali-free accelerators for high performance concrete, Gallerie e Grandi Opere Sotteranee 70 (2003) 51–58 (available from www.patroneditore.com).
[4] C. Paglia, F. Wombacher, H. Bohni, M. Sommer, An evaluation of the sulphate resistance of cementitious material accelerated with alkali-free and alkaline admixtures: laboratory vs field, Cement and Concrete Research 32 (4) (2002) 665–671.
[5] D. Sharrocks, Investing in new accelerators, Concrete Engineering International 2 (1998) 14–15 (available from www.concreteengineering.com).
[6] D. Zampini, A. Walliser, M. Oppliger, T. Melbye, C. Maltese, C. Pistolesi, G. Tansini, E. Portigliatti, E. Dal Negro, Liquid based set accelerating admixtures for sprayed concrete: a comparison between alkali-free and alkali-rich accelerators, Gallerie e Grandi Opere Sotteranee 72 (2004) 30–40.
[7] E. Hoek, Practical Rock Engineering, A.A. Balkema Publishers, Rotterdam, 2000.
[8] M. Sommer, F. Wombacher, T.A. Burge, Alkali-free setting and hardening accelerator, EP 1167317 B1, 2002.
[9] R. Lunkenheimer, J. Breker, I. Potencsik, H. Altman, R. Sedelies, Solidifying and Hardening Accelerators for Hydraulic Binders, EP 946451 B1, 1999.
[10] prEN 934-5, Admixtures for concrete, mortar and grout — Part 5: admixtures for sprayed concrete — definitions, requirements, conformity, marking and labelling, CEN/TC 104 — Concrete and related products.
[11] Austrian Society for Concrete, Construction Technology, Guideline Sprayed Concrete, Vienna, 2004 July (available from www.concrete-austria.com).
[12] C. Maltese, C. Pistolesi, A. Bravo, T. Cerulli, D. Salvioni, M. Squinzi, Formation of nanocrystals of AFt phase during the reaction between alkali-free accelerators and hydrating cement: a key factor for sprayed concretes setting and hardening, in: Y.R. De Miguel, A. Porro, P.J.M. Bartos (Eds.), Proc. of 2nd International Symposium on Nanotechnology in Constructions, Bilbao, Spain, 2005, pp. 329–338.
[13] N. De Belie, C.U. Grosse, J. Kurz, H.W. Reinhard, Ultrasound monitoring of the influence of different accelerating admixtures and cement types for shotcrete on setting and hardening behaviour, Cement and Concrete Research 35 (11) (2005) 2087–2094.
[14] Mapei S.p.A., Studio sulla solubilità delle fasi del sistema solfatico, Prova di Valutazione Rapida N. 200502, Unpublished results.
[15] K. Doskov, T.A. Bier, C. Wohrmeyer, Formulating dry-mix mortars with calcium aluminates cement, La Farge Calcium Aluminates, presented at the workshop on dry-mortars — St. Petersburg, 1999, April 13–15, Technical paper TP-GB-CH-LAF-03/99 available from www.lafarge.com.
[16] A.F.M. Barton, N.M. Wilde, Dissolution rates of polycrystalline samples of gypsum and orthorhombic forms of calcium sulphate by a rotating disc method, Transactions of the Faraday Society 67 (1971) 3590–3597.
[17] J. Kang, E. Sakai, J. Lee, M. Morioka, M. Daimon, Influence of calcium sulphates on the hydration of $3CaO{\cdot}Al_2O_3$, Inorganic Materials 6 (1999) 99–104.
[18] Y. Nakajima, T. Higaki, T. Goto, Influence of calcium sulphate on early hydration of cement paste containing superplasticizer, Semento Konkurito Ronbunshu 51 (1998) 288–293.
[19] H.F.W. Taylor, Cement chemistry, Thomas Telford Publishing, 1998, p. 212.
[20] A. Bravo, T. Cerulli, C. Maltese, C. Pistolesi, D. Salvioni, Effects of increasing dosages of an alkali-free accelerator on the physical chemical properties of a hydrating cement paste, in: V.M. Malhotra (Ed.), Proc. of 7th CANMET/ACI, Berlin, Germany, 2003, pp. 211–225.
[21] F.M. Lea, in: P.C. Hewlett (Ed.), Chemistry of cement and concrete, Fourth edition, 1998, p. 266.
[22] C. Paglia, F. Wombacher, H. Böhni, The influence of alkali-free and alkaline shotcrete accelerators within cement systems, Cement and Concrete Research 31 (6) (2001) 913–918.
[23] T.A. Burge, Mode of action of alkali-free sprayed shotcrete accelerators, in: Bernard (Ed.), Shotcrete: Engineering Developments, 2001, pp. 79–85, www.routledge.com.
[24] T. Cerulli, C. Pistolesi, C. Maltese, D. Salvioni, Alkali-rich and alkali-free accelerators for shotcrete: physical, chemical and mechanical effects on cement hydration, in: L. Jany, A. Nisperos (Eds.), Proc. of 24th ICMA, San Diego, California, 2002, pp. 1–17, available from www.cemmicro.org.
[25] H.E. Schwiete, U. Ludwig, P. Jager, Investigation in the system $3CaO–CaSO_4–CaO–H_2O$, Highway Research Board, Symposium on Structure of Portland Cement Paste and Concrete, Washington, 1966, pp. 353–367.
[26] I. Odler, Special inorganic cements, E and F.N. Spon Editors, 2000, p. 205.
[27] K.L. Scrivener, P.L. Pratt, Microstructural studies of the hydration of C_3A and C_4AF independently and in cement paste, British Ceramic Proceedings 35 (1984) 207–219.